frontiers in Ecology and Evolution

ORIGINAL RESEARCH
published: 17 March 2022
doi: 10.3389/fevo.2022.794287

Microstructural and Genetic Insights Into the Formation of the "Winter Diffusion Layer" in Japanese Pearl Oyster *Pinctada fucata* and Its Relation to Environmental Temperature Changes

Kei Sato[1,2†], Davin H. E. Setiamarga[3,4†], Hiroshi Yonemitsu[3] and Keita Higuchi[5]*

[1] Department of Earth Sciences, School of Education, Waseda University, Tokyo, Japan, [2] Institute of Liberal Arts and Science, Kanazawa University, Kanazawa, Japan, [3] Department of Applied Chemistry and Biochemistry, National Institute of Technology, Wakayama College, Wakayama, Japan, [4] The University Museum, The University of Tokyo, Tokyo, Japan, [5] Mikimoto Pearl Research Laboratory, Shima, Japan

OPEN ACCESS

Edited by:
Sylvain Marcellini,
University of Concepcion, Chile

Reviewed by:
Felipe Aguilera,
University of Concepcion, Chile
Frederic Marin,
Délégation Centre-Est (CNRS), France

***Correspondence:**
Kei Sato
ksato@staff.kanazawa-u.ac.jp

†ORCID:
Kei Sato
orcid.org/0000-0001-8308-1579
Davin H. E. Setiamarga
orcid.org/0000-0002-3854-4893

Specialty section:
This article was submitted to Evolutionary and Population Genetics, a section of the journal Frontiers in Ecology and Evolution

Received: 13 October 2021
Accepted: 21 January 2022
Published: 17 March 2022

Citation:
Sato K, Setiamarga DHE, Yonemitsu H and Higuchi K (2022) Microstructural and Genetic Insights Into the Formation of the "Winter Diffusion Layer" in Japanese Pearl Oyster Pinctada fucata and Its Relation to Environmental Temperature Changes. Front. Ecol. Evol. 10:794287. doi: 10.3389/fevo.2022.794287

Phenotypic plasticity in molluscan shell microstructures may be related to environmental changes. The "winter diffusion layer," a shell microstructure of the Japanese pearl oyster *Pinctada fucata,* is an example of this phenomenon. In this study, we used *P. fucata* specimens with shared genetic background to evaluate the seasonal plasticity of shell microstructures, at molecular level. To detect the seasonal changes in shell microstructure and mineral composition, shells of multiple individuals were periodically collected and analyzed using scanning electron microscopy and Raman spectrophotometry. Our observations of the winter diffusion layer revealed that this irregular shell layer, located between the outer and middle shell layers, had a sphenoid shape in radial section. This distinct shape might be caused by the internal extension of the outer shell layer resulting from growth halts. The winter diffusion layer could be distinguished from the calcitic outer shell layer by its aragonitic components and microstructures. Moreover, the components of the winter diffusion layer were irregular simple prismatic (the outer and inner sublayers) and homogeneous structures (the middle sublayer). This irregular formation occurred until April, when the animals resumed their "normal" shell formation after hibernation. To check for a correlation between gene expression and the changes in microstructures, we conducted qPCR of seven major biomineralization-related shell matrix protein-coding genes (*aspein*, *prismalin-14*, *msi7*, *msi60*, *nacrein*, *n16*, and *n19*) in the shell-forming mantle tissue. Tissue samples were collected from the mantle edge (tissue secreting the outer shell layer) and mantle pallium (where the middle shell layer is constructed) of the same individuals used for microstructural observation and mineral identification that were collected in January (winter growth break period), April (irregular shell formation period), and August (normal shell formation period). Statistically significant differences in gene expression levels were

observed between mantle edge and mantle pallium, but no seasonal differences were detected in the seasonal expression patterns of these genes. These results suggest that the formation of the irregular shell layer in *P. fucata* is caused by a currently unknown genetic mechanism unrelated to the genes targeted in the present study. Further studies using big data (transcriptomics and manipulation of gene expression) are required to answer the questions herein raised. Nevertheless, the results herein presented are essential to unravel the intriguing mystery of the formation of the winter diffusion layer, which may allow us to understand how marine mollusks adapt or acclimate to climate changes.

Keywords: biomineralization, shell matrix protein, shell microstructure, *Pinctada fucata*, winter diffusion layer, phenotypic plasticity, gene expression pattern, nacreous structure

INTRODUCTION

Biominerals are inorganic minerals precipitated by living organisms that are mainly used to form external hard structures (i.e., exoskeletons and shells) and internal hard tissues (i.e., endoskeletons) (Crenshaw, 1990). Such structures are composed of both minerals and minor organic matrix, and their formation and organization, including at the microscale (e.g., mineral composition, crystallographic axes, and microstructures), seem to be under genetic control, at least to some degree (Carter, 1990). The presence of an external, mineralized shell is one of the defining characteristics of mollusks (Kocot et al., 2016). Calcium carbonate-based biominerals (e.g., aragonite, calcite, and rarely vaterite) are the main components of molluscan shells (Spann et al., 2010; Frenzel and Harper, 2011). Shells are not uniform but composed of few superimposed layers that are characterized by different arrangements – defined as "shell microstructures" – of their elementary crystallites (Marin et al., 2012). Many studies admit that the shell construction in mollusks is an organic matrix-mediated process (Weiner et al., 1983): according to this view, cells or tissues secrete organic biomolecules that self-assemble in framework in which inorganic salts precipitate (Lowenstam, 1981).

Molecular studies on the genetics of shell formation (e.g., its microstructure and mineral composition) have been successful in identifying major shell matrix proteins (SMPs) such as Nacrein (Miyamoto et al., 1996), MSI60, and MSI31 (Sudo et al., 1997). Follow-up functional studies were also conducted to gain insights into their function in the regulation of microstructural formation and crystal polymorphism. For example, Suzuki et al. (2009) conducted knockdown on the Pif coding gene, and their experiment revealed that it is essential for nacre formation. To understand the involvement of Aspein in calcification, Takeuchi et al. (2008) conducted an *in vitro* $CaCO_3$ crystallization experiment, in which they found that it promotes calcite precipitation. Recent developments in gene and protein sequencing have allowed for the accumulation of data on complete gene sequences of novel shell proteins, their molecular evolution, and the comparison of analogs and homologs of various SMPs found in different species with similar shell microstructures (Marie et al., 2011, 2012, 2017; Isowa et al., 2012; Zhang et al., 2018; Setiamarga et al., 2021).

The results of above-mentioned biological studies have indicated that mollusks might have undergone a specific evolution in their shell mineralization process. However, these studies have not tackled the drastic microstructural evolutions that occurred throughout the geological periods. For example, such studies have targeted mollusk species with nacreous structures (mother of pearl) in their shells, partly due to scientific interests stemming from their commercial value. Originally, the nacreous structure was thought to be a symplesiomorphy in Conchiferan mollusks because it is present in the shell microstructures of the group's four major classes (Bivalvia, Gastropoda, Cephalopoda, and Monoplacophora). However, recent findings in paleontology indicate that the nacreous structure might have evolved independently in each class, and thus is probably a result of convergence (Checa et al., 2009; Vendrasco et al., 2011, 2013). Moreover, a recent phylogenetic study of Sato et al. (2020a) showed that in Protobranch bivalves (a basal taxon of bivalves), the nacreous structure was repeatedly lost in various lineages. Most Protobranch lineages that have lost the nacre tend to show a homogeneous structure. A similar pattern of shell microstructural evolution (nacre to homogeneous) was also found in Thraciid bivalves (Anomalodesmata) (Taylor et al., 1973). These examples suggest that even within a class, the nacreous structure is probably not homologous. From group to group, crystallographic variations in the crossed lamellar structure, another major molluscan shell microstructure, may also indicate convergent evolution (Kogure et al., 2014).

Moreover, phenotypic plasticity in the microstructures of molluscan shells among different individuals of the same lineage/species was also observed. One such variation is the thermal dependence of the crystallization and shell microstructures. For example, Höche et al. (2021) reported variations in crystal size in *Arctica islandica* shells depending on water temperature. Füllenbach et al. (2014) reported that the first-order lamellar orientation of the crossed lamellar structure in the freshwater gastropod *Viviparus viviparus* becomes uniform in stable and warm conditions. Gilbert et al. (2017) also reported thermal dependence in the thickness of molluscan nacre tablet crystals. Moreover, variations in the shell microstructure were reported by Lutz and Clark (1984: *Geukensia demissa*) and Nishida et al. (2012, 2015: *Scapharca*

broughtonii). Other than thermal dependence variation, Carter et al. (1998) reported nested occurrences of aragonitic and calcitic microstructures within the same shell layers in some bivalves, which were probably related to habitat conditions. A similar phenomenon was later confirmed by Sato et al. (2020b) in Pectinodontid limpets.

Most of the aforementioned reports on microstructural plasticity were studied in nacreless species. However, a similar phenomenon was observed for species with nacre. Moini et al. (2014) observed that *Nautilus pompilius* in aquaria forms shells with a disordered crystalline structure. Moreover, unique microstructures were observed from the repaired shells of nacre-bearing species (e.g., *Mytilus edulis*, Suzuki and Uozumi, 1979; *Haliotis tuberculata*, Fleury et al., 2008), suggesting that the molluscan mantle is originally capable of controlling microstructural plasticity. A similar phenomenon was also described in the Japanese pearl oyster *Pinctada fucata* by Wada (1961); he reported the formation of the "winter diffusion layer," a layer in the shell microstructure showing an irregular formation of mineral crystals formed only in winter, although he did not provide detailed images. These examples imply that the physiological condition of an animal, which in most cases occurs as a response to environmental changes, might somehow affect shell formation at the microstructural level.

The margaritid Japanese pearl oyster, *P. fucata*, is an important aquaculture species that has been industrially raised and cultured because of its pearl. However, it has been further developed as a model system for biological research, with its whole genome sequenced and published recently (Takeuchi et al., 2012, 2016). Some studies on *P. fucata* have focused on the molecular evolution of its genes (Koga et al., 2013; Setiamarga et al., 2013). The species has also been used as a model organism in several molluscan biomineralization studies (Suzuki et al., 2009). Thus, not only because of the availability of experimental tools, protocols, and a breadth of biological data, but also because it also has a winter diffusion layer, whose formation is probably related to low temperatures in winter, *P. fucata* is an appropriate model system for studying the mechanisms of seasonal phenotypic plasticity in the shell microstructure.

To our knowledge, no study has explicitly addressed the effect of low temperature on gene expression to explain the genetic mechanisms behind the formation of the winter diffusion layer. Therefore, in this study, we focused on the formation of the winter diffusion layer in *P. fucata* and examined its shell microstructure in samples taken in time series throughout the year. We also obtained mantle tissue samples from various months corresponding to seasonal changes throughout the year, and studied the expression patterns of seven shell matrix protein-coding genes. Our study on the expression of the shell matrix protein-coding gene in time series samples allows us to determine whether there is a correlation between possible fluctuations in gene expression and water temperatures caused by seasonal changes, and thus, a glimpse into the mechanisms of microstructural phenotypic plasticity in nacre-bearing Conchiferan mollusks. This also allows us to discuss the possible implications for the evolution of the biomineralized shell in mollusks.

MATERIALS AND METHODS

Materials

This study examined cultured individuals of the Japanese pearl oyster, *P. fucata*, at the MIKIMOTO Pearl Research Laboratory (Mie Prefecture, Japan). Pearl oysters in this institution are bred for commercial purposes. Our specimens were chosen at random from a single congenic breed to standardize their genetic background and placed in Ago Bay in front of the laboratory.

Pinctada fucata has a nacroprismatic shell; the outer shell layer has a calcitic columnar regular simple prismatic structure, the middle layer is of a sheet nacreous structure, the myostracum layer has an irregular simple prismatic structure, and the inner layer is again of a sheet nacreous structure (Taylor et al., 1969; Carter and Sato, 2020). Following the description of Wada (1961, 1972), the seasonal cycle of nacre formation in Japanese pearl oysters was defined for descriptive purposes as follows: (1) Winter growth break: shell formation in *P. fucata* ceases when the seawater temperature falls below 14°C; (2) Brief period of irregular shell formation: *P. fucata* resumes shell formation once the water temperature increases above 14°C; and (3) the normal nacroprismatic shells are secreted at a proper temperature (normal shell formation period). Wada (1961) mentioned that during the period of irregular shell formation, the middle and inner shell layers consist of incondite crystals called "a winter diffusion layer," although their microstructural diagnosis was unclear. Thus, to describe these incondite nacre crystals in detail and then evaluate intraspecific variations in the gene expression profile of the SMPs, five individuals of *P. fucata* were collected at each of the following dates: January 26 (winter growth break period), April 4 (irregular shell formation period), and August 2 (normal shell formation period), 2018. The seawater temperature at the sampling locality (2-m depth) was logged every 2 h on each collection date, and the daily averaged values were recorded as 11.0, 16.7, and 28.4°C, respectively (**Figure 1**). Samples were immediately dissected to collect mantle edges that secrete the calcitic columnar regular simple prismatic structure of the outer shell layer and interior parts of the mantle (mantle pallium), which is essential for the formation of the nacreous structure. Both parts were isolated from the dissected mantle piece based on the visual inspection of their color (mantle edge is brown and mantle pallium is faint yellow). Each mantle was cut into small (up to 5-mm square) pieces and fixed using RNA stabilization reagent (RNAlater, Qiagen, Hilden, Germany), and stored at –80°C until subsequent experiments. Remaining shells were used for shell microstructural observations and mineral identification. Furthermore, three shell samples were collected from each respective population at the end of each month from February to August 2018 for the observation of shell microstructures to assess the accurate period of the incondite nacre crystal formation and any individual specificities (see **Supplementary Table 1** for details of sample use).

Mantle Gene Expression Level Analysis

Total cellular RNA was isolated using the RNeasy Mini Kit (Qiagen, Valencia, CA, United States) from each mantle sample.

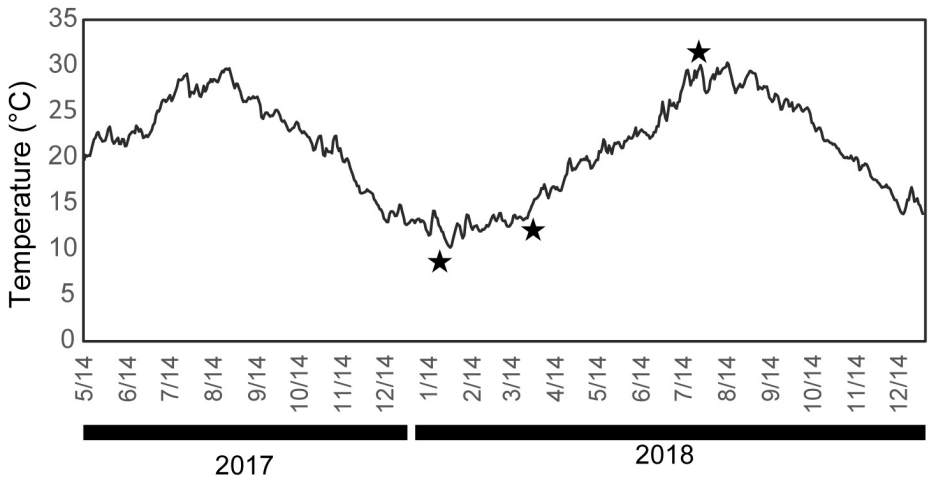

FIGURE 1 | Daily mean water temperature at the sampling point (2-m depth). Stars indicate the sampling dates (January 26, April 4, and August 2, 2018).

RNA was quantified, and its integrity was assessed using a NanoDrop Lite spectrophotometer (NanoDrop Technologies Inc., Wilmington, DE, United States). Then, reverse transcription was carried out using ReverTra Ace qPCR-RT Master Mix Kit (TOYOBO, Osaka, Japan) according to the manufacturer's instructions. The expression levels of seven biomineralization-related (*aspein*, *prismalin-14*, *msi7*, *msi60*, *nacrein*, *n16*, and *n19*) and two housekeeping genes (*gapdh* and *ef1α*) were analyzed by quantitative RT-PCR analysis using a set of forward and reverse primers (**Table 1**). *aspein* (Tsukamoto et al., 2004) and *prismalin-14* (Suzuki et al., 2004) are biomineralization-related shell matrix protein genes, which were discovered from the prismatic structure and are predominantly produced both at the mantle edge and center. Those discovered from nacreous structures such as *msi60* (Sudo et al., 1997), *nacrein* (Miyamoto et al., 1996), and *n16* (Samata et al., 1999) are dominant in the mantle pallium (Kinoshita et al., 2011). In addition, the gene expression level of *n19* (Yano et al., 2007), which is isolated from the nacreous structure, is moderate in the mantle center and high in the pearl sac (Wang et al., 2009). *msi7*, found by Zhang et al. (2003), is produced at both the mantle edge and center. The expression levels of the two housekeeping genes were analyzed to normalize the expression levels of the seven target genes based on the assumption that the expression levels of these housekeeping genes do not exhibit seasonal variation (Lee and Nam, 2016; Li et al., 2019). Quantitative PCR (qPCR) amplification using a Rotor-Gene SYBR Green PCR kit (Qiagen, Hilden, Germany) was carried out on a Rotor-Gene Q real-time PCR cycler (Qiagen, Hilden, Germany), using the following profile, based on the manufacturer's protocol: initial denaturation for 5 min at 95°C, followed by 40 cycles of denaturation for 5 s at 95°C and annealing/extension for 10 s at 60°C. After qPCR, the amplicon melting temperature curve was analyzed to confirm the absence of non-specific products (55–95°C with a heating rate of 1°C for each step, with continuous fluorescence measurement). The comparative threshold cycle (Ct) method was applied to analyze the expression levels of the examined genes using the Rotor-Gene Q Series Software ver. 2.0.2 (Qiagen, Hilden, Germany).

Statistics

Data distribution of the gene expression levels of SMPs from each of the five specimens collected in January, April, and August and two different parts of the mantle (mantle edge/mantle pallial) were analyzed using the Kolmogorov–Smirnov test and two-sample *t*-test, respectively. Then, a non-parametric Kruskal–Wallis test was applied to assess the significant differences among the three groups (January, April, and August). Statistical analyses were performed with EZR version 1.50 (Kanda, 2013), which is a graphical user interface for R version 4.0.2 (R Core Team, 2020), and the statistical tools in Microsoft Excel (version 2008).

Observations of Shell Microstructures and Determining Their Mineralogy

Miyamura and Makido (1958) confirmed that the characteristics of the pearl from various parts of the mantle are more continuous in *P. fucata* than in the freshwater pearl-producing bivalve (*Hyriopsis schlegeli*) (Mizumoto, 1965). Therefore, the posterodorsal parts of the shells were cut into small pieces (approximately 1 × 2 cm square) using a hand cutter and observed under a scanning electron microscope (SEM, Hitachi-S3400N, Tokyo, Japan). The left valves were used for most specimens, but the right valve was used in one specimen (sample ID: 180802-1). Both the inner shell surfaces and polished planes of the radial section of the shells were observed to characterize the shell microstructures around the mineralization front of the nacreous layer (i.e., the boundary between the outer and middle shell layers). The polished planes were filled with epoxy resin (Crystal Resin II super clear, Nisshin Resin Co., Kanagawa, Japan) before cutting using a low-speed saw (Minitom, Struers, Copenhagen, Denmark) and were prepared using a graded series of carborundum powder. After these processes, they were treated through: (1) removal of organic matter contained in the shell

TABLE 1 | Nucleotide sequences of primers used in real-time PCR.

Primer name		Sequence	References
Prismalin14	Forward primer	ATTTCCCGCGTTTCTCCTAT	Takeuchi and Endo, 2006
	Reverse primer	CCTCCGTAACCACCGTTAAA	Takeuchi and Endo, 2006
Aspein	Forward primer	TACTTTCCCAGTGGCTGACC	Takeuchi and Endo, 2006
	Reverse primer	CATCACTGGGCTCCGATACT	Takeuchi and Endo, 2006
MSI7	Forward primer	GATAAAAGGTCGGTGCCCAAC	Zhang and He, 2011
	Reverse primer	AAGGTTGATGCCAGGTCCGTA	Zhang and He, 2011
N16	Forward primer	CTCATACTGCTGGATACCCTACGA	Miyazaki et al., 2010
	Reverse primer	TCATTCCACATCTAAGCCACTCA	Miyazaki et al., 2010
N19	Forward primer	TGGCAACAAAGCAGTCATAACCG	Zhang and He, 2011
	Reverse primer	GGCGTCGTTGTAGCATTGAAGG	Zhang and He, 2011
MSI60	Forward primer	GATCTCCCCACACAACATAGATAGAG	Miyazaki et al., 2010
	Reverse primer	TGAATTGAAGCCTAATACTGGTCTGT	Miyazaki et al., 2010
Nacrein	Forward primer	CTTCATTGCATGTGGAATTGGA	Miyazaki et al., 2010
	Reverse primer	TCGGTTCTGATGATTGGTCACT	Miyazaki et al., 2010
GAPDH	Forward primer	TATTTCTGCACCGTCTGCTG	Takeuchi and Endo, 2006
	Reverse primer	ATCTTGGCGAGTGGAGCTAA	Takeuchi and Endo, 2006
EF1-α	Forward primer	CCTGGCCACAGAGATTTCAT	Takeuchi and Endo, 2006
	Reverse primer	AATTCCCCAACACCAGCAG	Takeuchi and Endo, 2006

with sodium hypochlorite for 30 min, and (2) etching with 0.2% (vol/vol) HCl for 1 min. The surfaces of the polished planes were coated with gold, but some were re-polished after SEM observation or not coated for mineral identification. Raman spectroscopy (inVia RefreX, Renishaw) was used to determine the calcium carbonate phase of the irregular shell layer, using a 532-nm laser with a holographic notch filter as a laser excitation source. The shell surfaces were carefully observed using SEM prior to Raman analysis to verify the position of the irregular shell layer. Each layer was marked by carbon adhesive tape or felt pen immediately after SEM observation (see **Figures 2A,C**). These landmarks were corrected by repeated SEM observations, and minor amendments of their positions were performed. The regions of interest were selected through SEM imaging and subsequently analyzed with Raman spectroscopy. Several spots in a single sample were analyzed to identify the mineralogy of each shell layer. The Raman peaks were identified based on Kontoyannis and Vagenas (2000).

RESULTS

Shell Microstructure Surrounding the Nacre Growth Front

Scanning electron microscope images obtained from the small pieces of *P. fucata* shells collected monthly from January to August 2018 are shown in **Figures 3–5**. Outer calcitic columnar regular simple prismatic and middle sheet nacreous structures were observed in all specimens, and the outer prismatic structure was composed of wide prominent first-order prisms (more than 20 μm on average) perpendicularly aligned to the shell surface (**Figures 3A,B**). Each prism was filled with second-order fine granular to lamella crystals (**Figure 3C**) and ensheathed by the organic wall. Second-order lamella crystals were stacked horizontally or obliquely to the shell surface, and their angle changed depending on the prism (**Figure 3C**). A thin layer (<20 μm in thickness), the so-called initial nacreous layer (Dauphin et al., 2008; Saruwatari et al., 2009), was inserted between the prismatic and nacreous structures in all the observed specimens (**Figure 3C**). This layer was the aggregation of hemispherical prisms with second-order irregularly shaped acicular crystals radiating from the center of the hemisphere (high-angle non-denticular composite prismatic structure). The middle sheet nacreous structure consisted of flattened polygonal column-to-circular cylindrical tablets stacked vertically to the shell surface (**Figures 3D–I**). Their bottom shape varied according to the individuals and/or dorsoventral axes (i.e., the mineralization front of the nacre to the thickened part of the middle shell layer). Regarding the bottom morphology of the nacre tablets near the mineralization front, their shape changed from circular to elliptic from winter to summer (**Figures 3E,F,H,I**).

Another thin sphenoid layer in the radial shell section often lied next to the initial nacreous layer (**Figures 4**, **5**) in the area where the outer prisms were discontinued in a wedge shape (**Figures 4A,D,G,H**). Aragonite was detected in this layer (sample ID 180226-1, **Figures 4A–C**) using Raman spectrometry (**Figure 2**). This layer comprised three components: a middle sublayer consisting of fine-grained crystals (less than 1 μm in diameter) sandwiched between the outer and inner sublayers of irregularly shaped acicular crystals (**Figures 4C,E,I**). The boundary of the initial nacreous layer was sometimes difficult to identify (**Figures 4B,E**). The middle sublayer sometimes did not appear depending on the specimens (aragonitic simple prismatic structure; **Figures 4G,H**). Organic walls stood perpendicular to the shell surface and surrounded the crystals irregularly in this layer at the side close to the outer shell layer (**Figures 4B,E,I**); moreover, they decreased distal to the outer shell layer

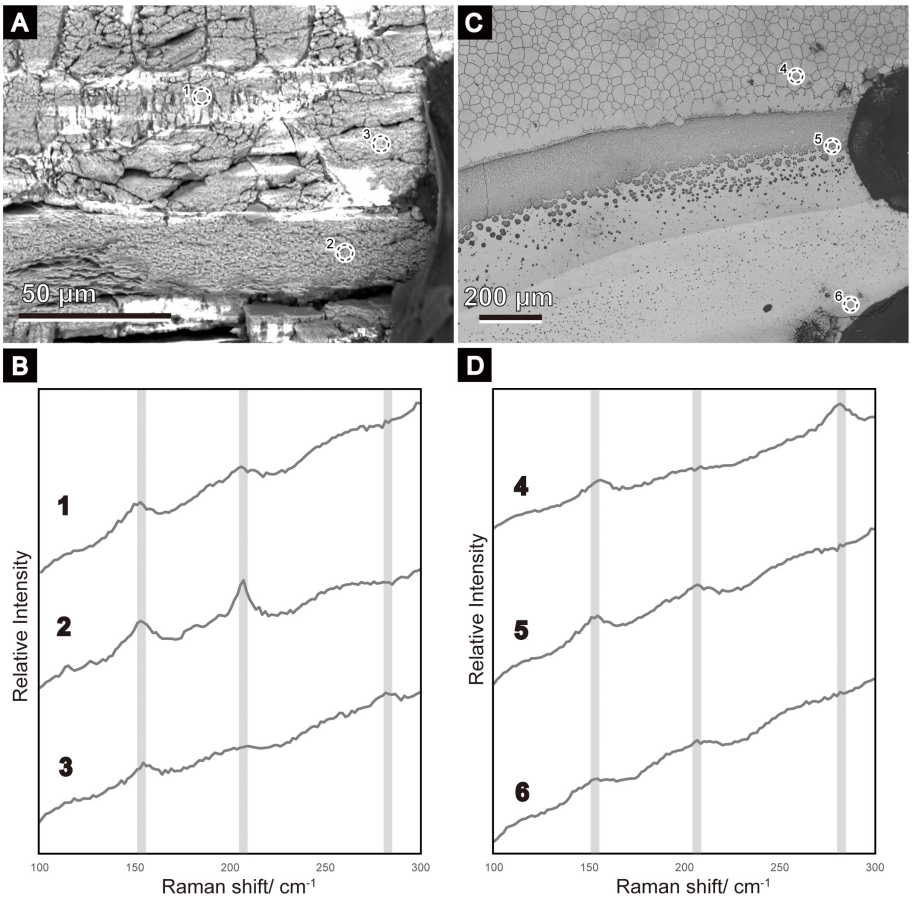

FIGURE 2 | Scanning electron micrographs **(A,C)** of the areas where Raman analyses were conducted, and the resulting Raman spectra **(B,D)**. The broken-lined circle roughly indicates the part from which the Raman spectra were acquired (1–6). **(A)** Radial section of ID 180226-1. A similar position before re-polishing to remove evaporated gold for Raman analysis is shown in **Figure 4B**. A carbon tape was attached to the right as a landmark. **(B)** Inner shell surface of ID 180226-1 (**Figure 5A**). Dots on the right side were used as landmarks. **(B,D)** Raman spectra of calcitic columnar regular simple prismatic structures are indicated by 3 and 4; the sheet nacreous structure is indicated by 2; the winter diffusion layers are indicated by 1, 5, and 6. Aragonite peaks (152, 205) are clear in 1, 2, 5, and 6, whereas calcite peaks (154, 280) are detected in 3 and 4.

(**Figure 4A**). As a result, the appearance of irregular pits (**Figures 5C,E**) at the inner shell surfaces also decreased toward the dorsal side in the middle sublayer, and then this sublayer became analogous to the homogeneous structure because it had no apparent structural unit (**Figures 4C**, **5C**). Discontinued and irregular networks of organic walls (**Figure 5B**) and adjoined or collapsed nacre tablet-shaped prisms (**Figures 5F,G**) were observed on the inner shell surfaces of the outer and inner sublayers. This layer appeared in the inner shell surface of specimens collected from February to April, but it was distant from the nacre mineralization front of the remaining specimens (collected from May to August).

Expression Patterns of Shell Matrix Protein Genes

The expression levels of the seven biomineralization-related genes were analyzed using quantitative real-time PCR (qPCR) (**Figure 6**). Statistically significant differences were observed between mantle edge and mantle pallium in the expression levels of *n16*, *msi60*, and *aspein* in *ef1*α normalized data and of *n16*, *nacrein*, and *aspein* in *gapdh* normalized data. Although not statistically significant, the expression levels of *msi60*, *n16*, and *n19* were higher in mantle pallium than in mantle edges in all three groups (collected in January, April, and August). Conversely, *aspein* and *prismalin-14* were generally expressed significantly in the mantle edge. The expression levels of *nacrein* and *msi7* in the mantle exhibited no clear statistical significances.

Regarding seasonal expression patterns, no statistically significant pattern was noted in any of the analyzed genes. Nonetheless, *msi60* and *n16* expression patterns were lower in April. *n19* had the highest expression levels in the mantle pallium of January individuals and the second-highest in those of April individuals. April individuals had the lowest expression of *prismalin-14* and *aspein* in the mantle edge when considering *ef1*α-normalized data, but their expression was lowest in August individuals considering *gapdh*-normalized data. When considering *ef1*α-normalized data, *nacrein* expression

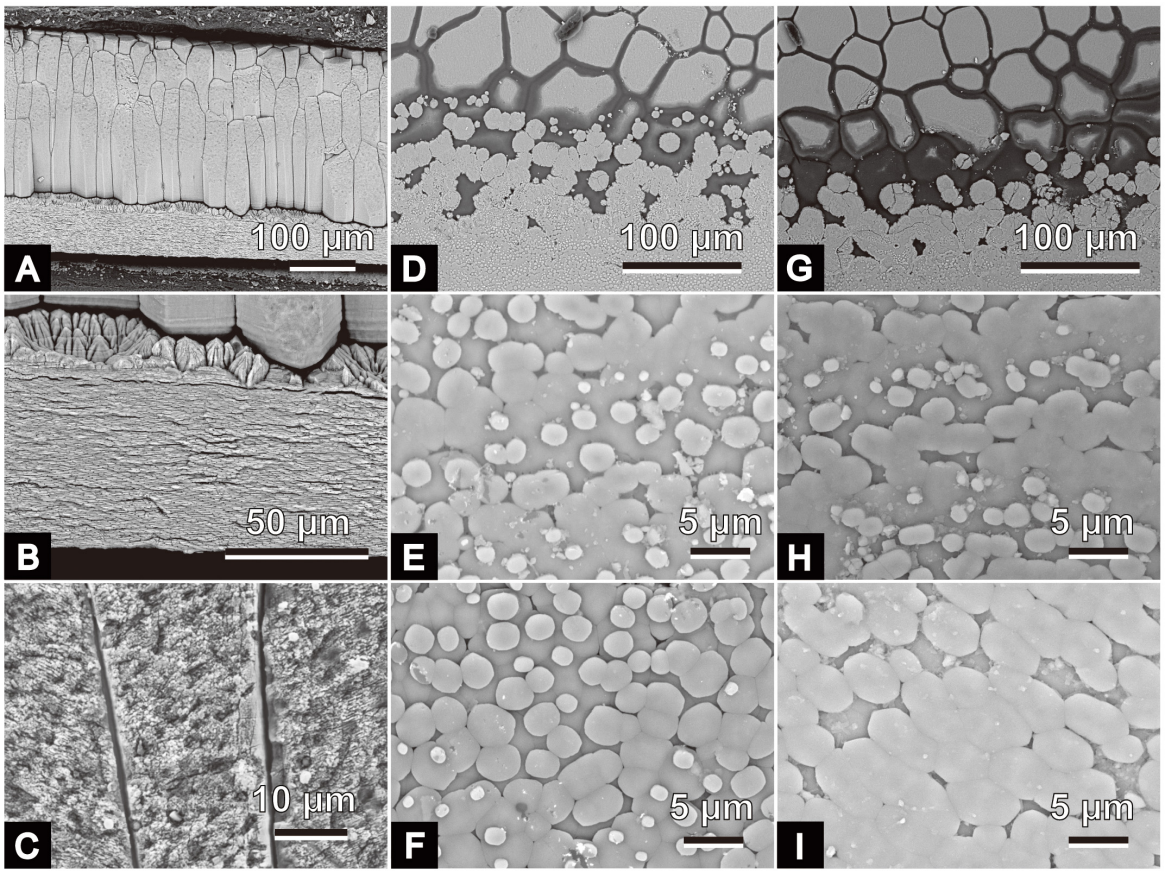

FIGURE 3 | Scanning electron micrographs of microstructures of *Pinctada fucata*. **(A–C)** Radial sections of the polished plane. Growth directions (i.e., direction of the shell margin) are on the right side. **(A)** Outer calcitic columnar regular simple prismatic to middle sheet nacreous structures of a specimen collected on June 26, 2018 (ID: 180626-1). **(B)** Detailed view of panel **(A)**; a thin initial nacreous layer is visible between the outer and middle shell layers. **(C)** Detailed view of the outer shell layer of specimen collected on January 26, 2018; ID: 180126-5). **(D–I)**: growth front of nacre on the inner surfaces and the upper sides of these images indicate the direction of the shell margins. **(D,E)** Specimen collected on May 28, 2018, ID: 180528-1. **(F)** Specimen collected on June 26, 2018, ID: 180626-1; **(G,H)**. Specimen collected on July 25, 2018, ID: 180725-1. **(I)** Specimen collected on August 2, 2018, ID: 180802-1. The outer calcitic columnar regular simple prismatic structure and the middle sheet nacreous structure appear on the upper and lower sides of panels **(D,G)**, respectively.

levels showed a trend similar to those of *msi60* and *n16* in the mantle pallium, with April individuals having the lowest expression levels; however, no clear trend was noted for *nacrein* expression levels when considering *gapdh*-normalized data. The expression levels of *msi7* were the lowest in August.

DISCUSSION

Diagnosis of the Irregular Shell Layer

We carefully described the microstructural characteristics of the irregular shell layer formed within the sheet nacreous structure of the middle shell layer. This layer was found on or close to the inner shell surfaces of cultured *P. fucata* individuals collected from February to April. We consider this seasonal formation to be analogous to that of the "winter diffusion layer" reported by Wada (1961). Our analysis revealed that this irregular layer (1) has a sphenoid shape in the radial section of the shell, (2) is found between the initial and regular nacreous layers, (3) is aragonitic (**Figure 2**), and (4) is composed of three sublayers: outer and inner layers of irregular simple prismatic structures, and middle layer with homogeneous to aragonitic simple prismatic structures (**Figures 4**, **5**). Wada (1961) described the "winter diffusion layer" as being composed of four components: (1) a granular layer constructed before hibernation, (2) a roughened surface resulting from shell dissolution during hibernation, (3) a conchiolin layer constructed immediately after the end of hibernation, and (4) a granular layer constructed after hibernation. The difference between our observations and those of Wada (1961) probably results from the method used, as the latter was mainly conducted on the inner shell surface, which makes the microstructural diagnosis unclear. Although further verification is needed, the granular layers of Wada (1961) probably coincide with our irregular shell layer comprising three sublayers.

The sphenoid shape entering the outer shell layer herein shown is similar to the extension of the outer shell layer into the inner shell layer observed in some unioid bivalves (Checa, 2000). The irregularly layered unioid shells are considered to

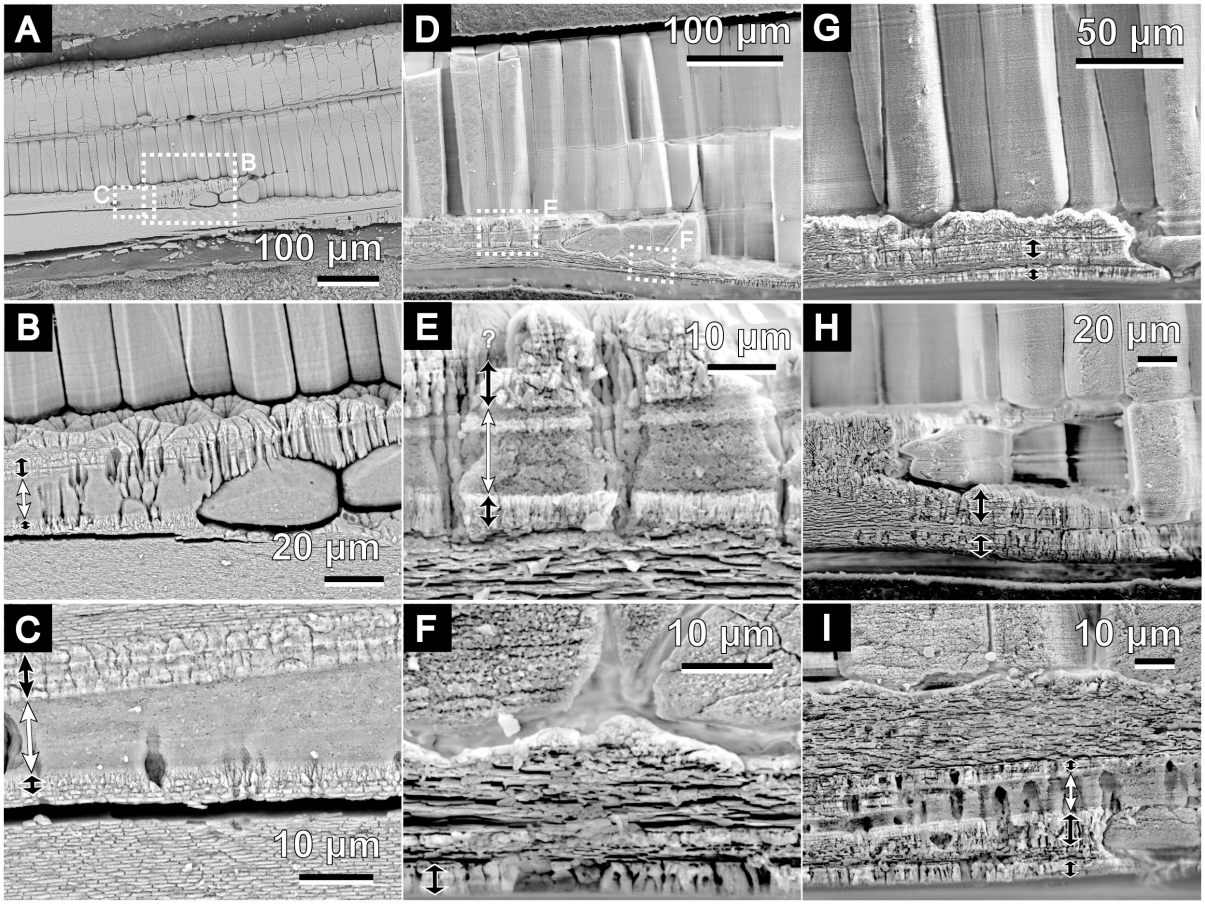

FIGURE 4 | Scanning electron micrographs of the microstructure of the irregular shell layer in *P. fucata*. All images show radial sections in polished planes. Growth direction of the shells are on the right side of images. White double-headed arrows indicate the middle sublayer of the irregular shell layer between the outer and middle layers. Black arrows show the distribution of the outer and inner sublayers. **(A)** Outer to middle shell layers of ID 180226-1, collected on February 26, 2018. Detailed views in panels **(B,C)**. **(D)** Outer to middle shell layers of ID 180404-4, collected on April 4, 2018. Detailed views in panels **(E,F)**. **(G–I)** Show the same structures as in panels **(A,D)**, but are of different individuals collected on April 4, 2018 [ID 180404-1 **(G)**, ID 180404-3 **(H)**, and ID 180404-2 **(I)**].

result from the retraction of the outer mantle fold during annual or semi-annual growth halts [see description by Checa (2000)]. Some arcid bivalves also have an annual sphenoid insertion of the composite prismatic structure into the crossed lamellar structure within the outer shell layer (Kobayashi, 1976a,b; Nishida et al., 2012). Nishida et al. (2015) experimentally confirmed that the variation in thickness of the composite prismatic structure was synchronized with water temperature. A similar physical reaction (i.e., retraction of the mantle due to the low water temperature) is likely to have occurred during the formation of the winter diffusion layer in *P. fucata*; therefore, this layer can be considered a unique type of annual disturbance ring.

Putative Mechanisms of Formation of the Winter Diffusion Layer

Genetic or epigenetic mechanisms might be a component in the formation of peculiar microstructures such as the winter diffusion layer. *In vitro* studies by Takeuchi et al. (2008), genetic manipulation studies by Suzuki et al. (2009), and other biochemical and physicochemical studies (e.g., Olson et al., 2012; Zhang et al., 2018) have strongly suggested that physics and chemistry cannot thoroughly explain the intricate mechanisms of biomineralization in living organisms. Meanwhile, several studies have also examined the expression of some shell matrix protein-coding genes in margaritid bivalves and found a correlation between gene expression patterns and variations in environmental conditions (e.g., food supply and high temperature) (Joubert et al., 2014; Latchere et al., 2017). We hypothesized that the expression pattern of SMPs changes at low temperature, leading to the formation of the winter diffusion layer.

We herein focused on the genes coding for SMPs as they are possibly directly related to the biomineralization process during shell formation, as shown by Suzuki et al. (2009) and Zhang et al. (2018). No information is available on the signaling pathway controlling the expression of SMP-coding genes. However, our working hypothesis was that this does

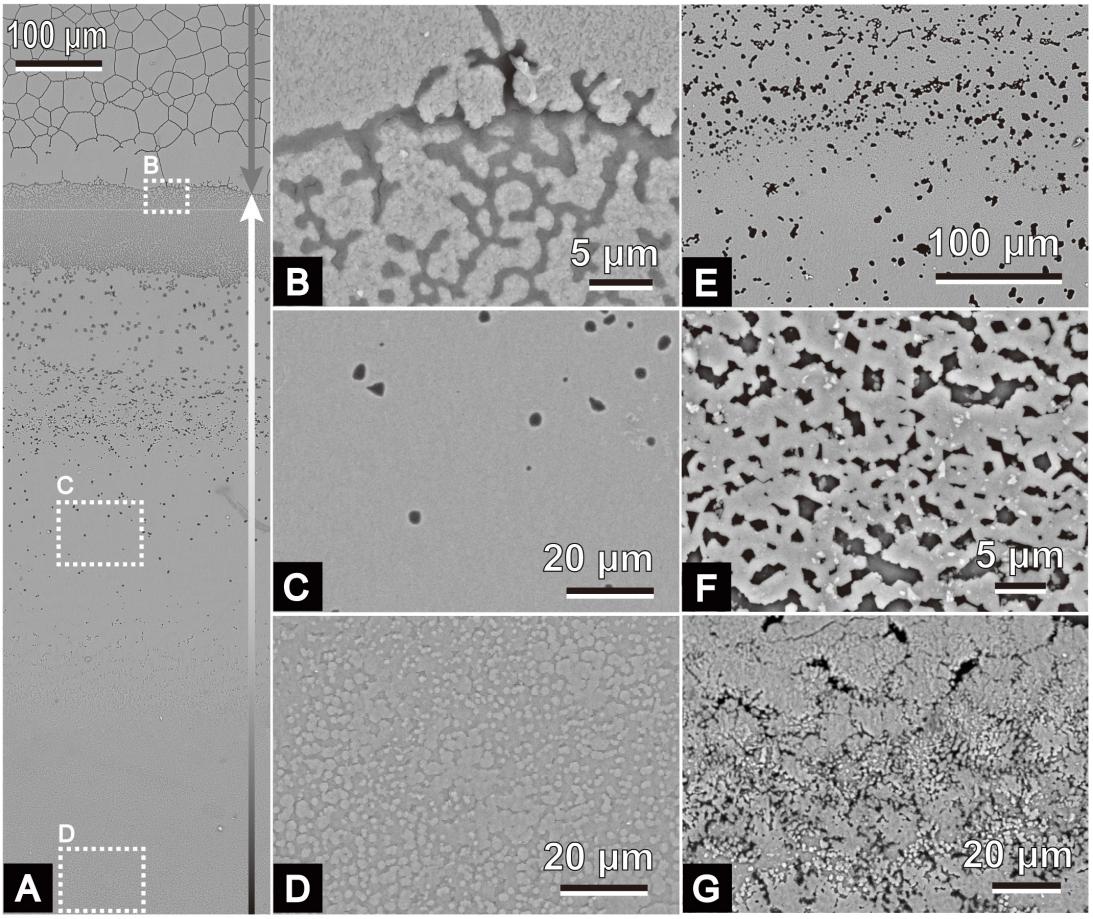

FIGURE 5 | Scanning electron micrographs of the microstructure of the irregular shell layer in *P. fucata*. All images show inner shell surfaces. Shell margins are on the upper sides of the images. **(A)** Inner shell surface of ID 180226-1, collected on February 26, 2018. Gray arrow indicates the outer calcitic columnar regular simple prismatic structure. The irregular shell layer covers the inner surface of the outer layer **(B,C)** and the middle sheet nacreous gradually accumulates **(D)** on it (indicated by the white and black arrow). Variations of the irregular shell layer are shown in panel **(E)** (ID 180424-1, collected on April 24, 2018), **(F)** (ID 180404-1, collected on April 4, 2018), and **(G)** (ID 180404-3, collected on April 4, 2018).

not matter because all upstream mechanisms controlling the expression of the SMP-coding genes must affect the expression of the SMP-coding genes themselves, with a possible feedback loop to the signaling pathways causing possible attenuation or suppression of the downstream genes controlling the phenotypes (Venturelli et al., 2012; Zhang et al., 2012; Liu et al., 2017). Changes in SMP-coding genes must then be translated into the actual biomineralization process. Thus, we examined the expression levels of seven biomineralization-related proteins in specimens collected in different seasons to cover the herein defined seasonal cycle of nacre formation (i.e., winter growth break, irregular shell formation, and normal shell formation). However, no statistical significance was detected in the SMP gene expression levels among seasons, which interestingly shows that these seven SMPs, although important for shell formation, are probably not affected by temperature changes, and are thus not involved in the formation of the winter diffusion layer of *P. fucata*. Nevertheless, whether changes in the expression levels of other SMPs with varying environmental factors influence the formation and irregularities of shell microstructures remains to be tested. Moreover, further experiments using samples cultured in a controlled environment to cancel other parameters (e.g., food supply) that could affect the gene expression of SMPs should be performed. Genetic mechanisms may also be indirectly involved in the formation of irregular microstructures. For example, the increased expression of housekeeping genes as a result of environmental cues might be involved in the subsequent induction of the appropriate expression of upstream genes (regulatory genes and transcription factors) related to development, growth, and cell proliferation (e.g., *dpp*) (Rogulja and Irvine, 2005; Shimizu et al., 2013) or to direct metabolic and physiological responses to such changes (Shinomiya et al., 1999). Although the stability of the expression of downstream genes such as the SMP-coding genes is controlled by homeostasis (as is also suggested by our results), cells expressing SMPs are either physically or chemically different as they respond to environmental cues, which in turn may cause variations in their phenotypes.

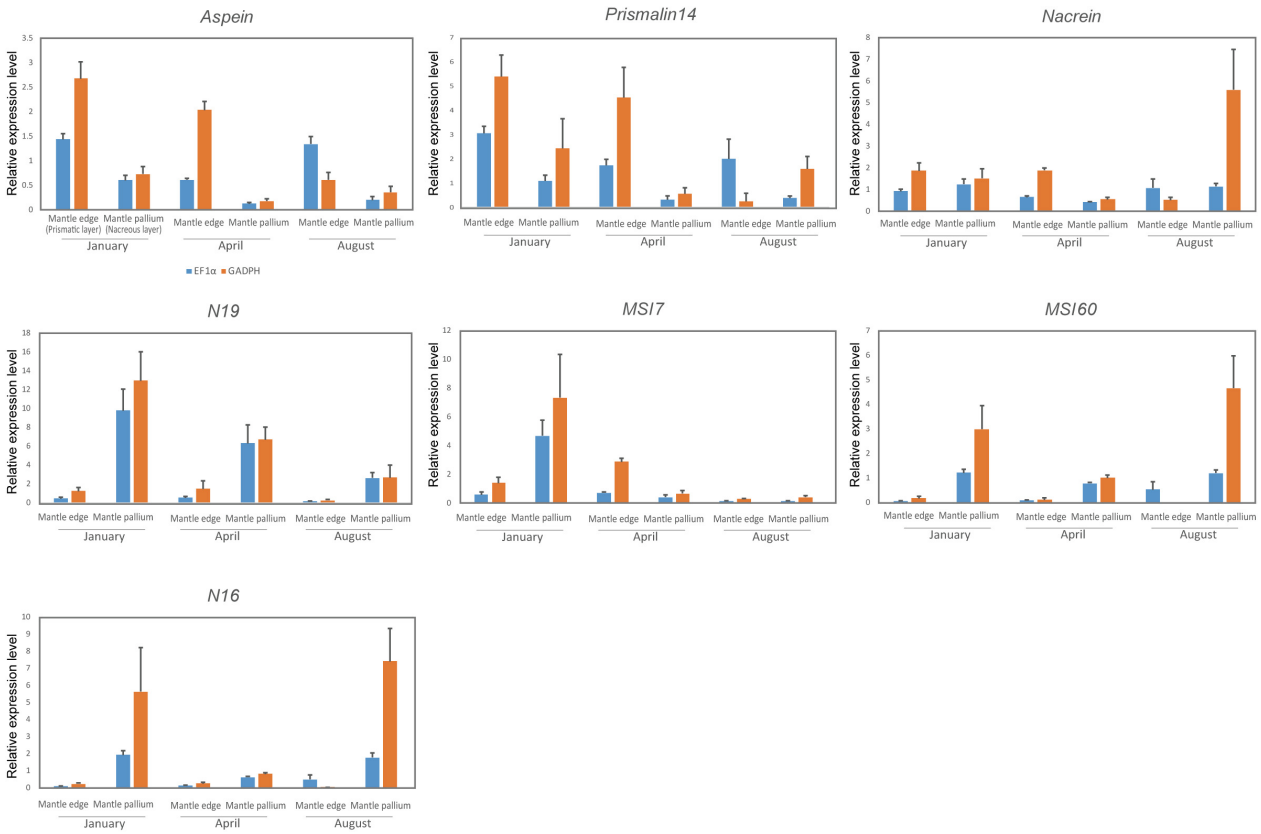

FIGURE 6 | Relative gene expression of biomineralization-related shell matrix genes normalized by housekeeping genes (blue, EF1α; orange, *GAPDH*). Each value represents the mean ± SD of the data analyzed on up to five individuals.

The thermodynamic process is another candidate driving force of the formation of the winter diffusion layer. Olson et al. (2012) hypothesized that the crystallographic axes and morphology of nacre crystals could be related to environmental factors (water temperature and pressure), and Gilbert et al. (2017) demonstrated that the thickness of nacre tablets is correlated with water temperature. Both studies attributed these changes to thermodynamics, whereas Cartwright et al. (2020) considered that changes in nacre thickness were rather a type of biological control determined by the position of the interlamellar membranes, which are secreted before nacre formation. Olson et al. (2012) and Gilbert et al. (2017) also hypothesized that the addition of some proteins to chitin nanocrystals affects the thermally dependent thickening of nacre tablets, besides suggesting the existence of gaps in the knowledge on the role of SMPs on nacre thickness and irregular shell formation, which could be driven by other genetic mechanisms involving transcription factors, cell metabolism-controlling genes, and other upstream genes. We herein observed that the interlamellar membranes surrounding the nacre tablets reduced and showed an irregular distribution or even disappeared, which may have resulted from the low expression of specific insoluble SMPs. Moreover, the downsized and deformed crystals were found in the winter diffusion layer. These may be linked to the change in calcium carbonate deposition and/or nucleation rate; or. from a biological perspective, they may have been caused by the inhibitory activity of SMPs on the crystallization of $CaCO_3$. SMPs other than those herein tested may be directly or indirectly involved in the formation of these microstructural changes. Furthermore, the time gap between our sampling and the animals' irregular shell formation and the number of individuals for statistical analysis should be considered in further studies.

Some of the SMP genes herein tested (*aspein*, *prismalin-14*, *n19*, and *msi7*) had higher expression in the mantle pallium of winter individuals, although these data were not statistically significant. These expression patterns were consistent with the development of nacre tablets. Wada (1972) showed that the (001) planes of aragonite in the middle and inner nacreous layers (i.e., basal planes of nacre tablets) became larger during winter until animal hibernation, when the calcification process was slow. This relationship between nacre growth and SMP expression may be statistically significant in a sampling period larger than that used in the present study. Therefore, future studies with DNA chip analysis and exhaustive exploration of the mantle transcriptome and shell proteomics might provide biological insights into the genetic mechanisms of the formation of the winter diffusion layer in *P. fucata* shells.

The Formation of the Irregular Shell Microstructures and Its Implication to Molluscan Shell Evolution

As previously mentioned, some Protobranchia and Thraciidae bivalves that presented a nacreous structure lost their nacreous shells and acquired a homogeneous structure mostly in the Paleozoic and Mesozoic (Taylor et al., 1973; Sato et al., 2020a). Many studies have suggested that the nacreous structure is costly and has gradually lost its "market share" in the course of molluscan evolution (Cartwright and Checa, 2007; Frýda et al., 2010; Vendrasco et al., 2013). Meanwhile, the similar appearance of a homogeneous structure with an irregular microstructure within the nacreous structure as in winter *P. fucata* has also been reported for *Nautilus pompilius* in the aquarium [see Figure 7 in Moini et al. (2014)]. The phenotypic plasticity of the shells in these two species seems to be triggered by adverse conditions, and may thus be a biological response to produce a low-cost shell. The production cost of molluscan shells can be estimated from their organic content (Palmer, 1992), and the homogeneous structure is presumed to be a low-cost material compared to the nacreous structure (Taylor and Layman, 1972). Consequently, the biomineralization mechanism that controls the phenotypic plasticity from a nacreous to a homogeneous structure also seems to drive shell microstructural evolutions. Therefore, in addition to exploring the genes involved in the formation of the irregular structure of the winter diffusion layer in *P. fucata*, assessing the homology between SMP genes in the homogeneous structure of mollusks (e.g., protobranchs) should be tackled in future paleobiological studies.

DATA AVAILABILITY STATEMENT

The original contributions presented in the study are included in the article/**Supplementary Material**, further inquiries can be directed to the corresponding author.

AUTHOR CONTRIBUTIONS

KS conceived the idea of this study and diagnosed the shell microstructure. KS, DS, and KH conducted the field sampling. KS, DS, and HY performed the gene expression experiments. KS and DS wrote the manuscript. All authors contributed to the discussion and interpretation of the data and read, edited, commented, and confirmed the content of the final version of this manuscript.

FUNDING

This research was supported by Grants-in-Aid for Scientific Research (21K14033) from the Japan Society for the Promotion of Science and Environment Research and Technology Development Fund (5RF-2101) of the Environmental Restoration and Conservation Agency of Japan to KS. DS was partially supported by FY2016 Research Grant for Chemistry and Life Sciences from The Asahi Glass Foundation, Grants-in-Aid for Scientific Research (C) (18K06363), and Grants-in-Aid for Exploratory Research (19K21646). This study was supported by the members of MIKIMOTO Pearl Research Laboratory (MPRL).

ACKNOWLEDGMENTS

We are especially grateful to Kiyohito Nagai and Yasunori Iwahashi for granting us permission to conduct this project in MPRL, besides giving us valuable technical advice. Takenori Sasaki gave technical advice on the anatomy of our sampling. Kazuyoshi Endo gave us valuable advice regarding the direction of our research. Keisuke Shimizu (University of Tokyo) and Akito Ishikawa (University of Tokyo) supported our molecular biology experiments and statistical analyses. Kozue Nishida (Tsukuba University) also gave valuable advice on our statistical analyses. We also thank the members of Setiamarga laboratory [National Institute of Technology (KOSEN), Wakayama College] for their assistance in setting up the environment for our experiments.

SUPPLEMENTARY MATERIAL

The Supplementary Material for this article can be found online at: https://www.frontiersin.org/articles/10.3389/fevo.2022.794287/full#supplementary-material

Supplementary Table 1 | Specimens used for qPCR and shell microstructural observation.

REFERENCES

Carter, J. G. (1990). *Skeletal Biomineralization: Patterns, Processes and Evolutionary Trends*, Vol. I. New York, NY: Van Nostrand & Reinhold.

Carter, J. G., and Sato, K. (2020). Part N, Revised, Chapter 2A: bivalve shell microstructure and mineralogy: shell microstructure terminology. *Treatise Online* 1, 1–81.

Carter, J. G., Barrera, E., and Tevesz, M. J. S. (1998). Thermal potentiation and mineralogical evolution in the bivalvia (Mollusca). *J. Paleontol.* 72, 991–1010.

Cartwright, J. H. E., and Checa, A. G. (2007). The dynamics of nacre self-assembly. *J. R. Soc. Interface* 4, 491–504. doi: 10.1098/rsif.2006.0188

Cartwright, J. H. E., Checa, A. G., and Sainz-Díaz, C. I. (2020). Nacre is a liquid-crystal thermometer of the oceans. *ACS Nano* 14, 9277–9281. doi: 10.1021/acsnano.0c05353

Checa, A. (2000). A new model for periostracum and shell formation in Unionidae (Bivalvia, Mollusca). *Tissue Cell* 32, 405–416. doi: 10.1054/tice.2000.0129

Checa, A. G., Ramírez-Rico, J., González-Segura, A., and Sánchez-Navas, A. (2009). Nacre and false nacre (foliated aragonite) in extant monoplacophorans (=Tryblidiida: Mollusca). *Naturwissenschaften* 96, 111–122. doi: 10.1007/s00114-008-0461-1

Crenshaw, M. A. (1990). "Biomineralization mechanisms," in *Skeletal Biomineralization: Patterns, Processes and Evolutionary Trends*, Vol. I, ed. J. G. Carter (New York, NY: Van Nostrand & Reinhold), 1–3.

Dauphin, Y., Ball, A. D., Cotte, M., Cuif, J. P., Meibom, A., Salomé, M., et al. (2008). Structure and composition of the nacre-prisms transition in the shell of *Pinctada margaritifera* (Mollusca, Bivalvia). *Anal. Bioanal. Chem.* 390, 1659–1669. doi: 10.1007/s00216-008-1860-z

Fleury, C., Marin, F., Marie, B., Luquet, G., Thomas, J., Josse, C., et al. (2008). Shell repair process in the green ormer *Haliotis tuberculata*: a

histological and microstructural study. *Tissue Cell* 40, 207–218. doi: 10.1016/j.tice.2007.12.002

Frenzel, M., and Harper, E. M. (2011). Micro-structure and chemical composition of vateritic deformities occurring in the bivalve *Corbicula fluminea* (Müller, 1774). *J. Struct. Biol.* 174, 321–332. doi: 10.1016/j.jsb.2011.02.002

Frýda, J., Klicnarová, K., Frýdová, B., and Mergl, M. (2010). Variability in the crystallographic texture of bivalve nacre. *Bull. Geosci.* 85, 645–662. doi: 10.3140/bull.geosci.1217

Füllenbach, C. S., Schöne, B. R., and Branscheid, R. (2014). Microstructures in shells of the freshwater gastropod *Viviparus viviparus*: a potential sensor for temperature change? *Acta Biomater.* 10, 3911–3921. doi: 10.1016/j.actbio.2014.03.030

Gilbert, P. U. P. A., Bergmann, K. D., Myers, C. E., Marcus, M. A., DeVol, R. T., Sun, C. Y., et al. (2017). Nacre tablet thickness records formation temperature in modern and fossil shells. *Earth Planet Sci. Lett.* 460, 281–292. doi: 10.1016/j.epsl.2016.11.012

Höche, N., Walliser, E. O., de Winter, N. J., Witbaard, R., and Schöne, B. R. (2021). Temperature-induced microstructural changes in shells of laboratory-grown *Arctica islandica* (Bivalvia). *PLoS One* 16:e0247968. doi: 10.1371/journal.pone.0247968

Isowa, Y., Sarashina, I., Setiamarga, D. H. E., and Endo, K. (2012). A comparative study of the shell matrix protein aspein in pterioid bivalves. *J. Mol. Evol.* 75, 11–18. doi: 10.1007/s00239-012-9514-3

Joubert, C., Linard, C., Le Moullac, G., Soyez, C., Saulnier, D., Teaniniuraitemoana, V., et al. (2014). Temperature and food influence shell growth and mantle gene expression of shell matrix proteins in the pearl oyster *Pinctada margaritifera*. *PLoS One* 9:e103944. doi: 10.1371/journal.pone.0103944

Kanda, Y. (2013). Investigation of the freely available easy-to-use software "EZR" for medical statistics. *Bone Marrow Transpl.* 48, 452–458. doi: 10.1038/bmt.2012.244

Kinoshita, S., Wang, N., Inoue, H., Maeyama, K., Okamoto, K., Nagai, K., et al. (2011). Deep sequencing of ESTs from nacreous and prismatic layer producing tissues and a screen for novel shell formation-related genes in the Pearl Oyster. *PLoS One* 6:e21238. doi: 10.1371/journal.pone.0021238

Kobayashi, I. (1976a). Internal structure of the outer shell layer *Anadara broughtnii* (Schrenck). *Venus* 35, 63–72.

Kobayashi, I. (1976b). The change of internal shell structure of *Anadara ninohensis* (Okuta) during the shell growth. *J. Geol. Soc. Japan* 82, 441–447.

Kocot, K. M., McDougal, C., and Degnan, B. M. (2016). "Developing perspectives on molluscan shells, part 1: introduction and molecular biology," in *Physiology of Molluscs: A Collection of Selective Reviews*, eds S. Saleuddin and S. Mukai (New York, NY: Apple Academic Press), 1–41. doi: 10.1201/9781315207483

Koga, H., Hashimoto, N., Suzuki, D. G., Ono, H., Yoshimura, M., Suguro, T., et al. (2013). A genome-wide survey of genes encoding transcription factors in Japanese pearl oyster *Pinctada fucata*: II. Tbx, Fox, Ets, HMG, NFκ;B, bZIP, and C2H2 Zinc Fingers. *Zoolog. Sci.* 30, 858–867. doi: 10.2108/zsj.30.858

Kogure, T., Suzuki, M., Kim, H., Mukai, H., Checa, A. G., Sasaki, T., et al. (2014). Twin density of aragonite in molluscan shells characterized using x-ray diffraction and transmission electron microscopy. *J. Cryst. Growth* 397, 39–46. doi: 10.1016/j.jcrysgro.2014.03.029

Kontoyannis, C. G., and Vagenas, N. V. (2000). Calcium carbonate phase analysis using XRD and FT-Raman spectroscopy. *Analyst* 125, 251–255. doi: 10.1039/a908609i

Latchere, O., Le Moullac, G., Gaertner-Mazouni, N., Fievet, J., Magré, K., and Saulnier, D. (2017). Influence of preoperative food and temperature conditions on pearl biogenesis in *Pinctada margaritifera*. *Aquaculture* 479, 176–187. doi: 10.1016/j.aquaculture.2017.05.046

Lee, S. Y., and Nam, Y. K. (2016). Evaluation of reference genes for RT-qPCR study in abalone Haliotis discus hannai during heavy metal overload stress. *Fish. Aquat. Sci.* 19, 1–11. doi: 10.1186/S41240-016-0022-Z

Li, Y., Zhang, L., Li, R., Zhang, M., Li, Y., Wang, H., et al. (2019). Systematic identification and validation of the reference genes from 60 RNA-Seq libraries in the scallop Mizuhopecten yessoensis. *BMC Genomics* 20:288. doi: 10.1186/s12864-019-5661-x

Liu, D., Albergante, L., and Newman, T. J. (2017). Universal attenuators and their interactions with feedback loops in gene regulatory networks. *Nucleic Acids Res.* 45, 7078–7093. doi: 10.1093/nar/gkx485

Lowenstam, H. A. (1981). Minerals formed by organisms. *Science* 211, 1126–1131. doi: 10.1126/science.7008198

Lutz, R. A., and Clark, G. R. (1984). Seasonal and geographic variation in the shell microstructure of a salt-marsh bivalve (*Geukensia demissa* (Dillwyn)). *J. Mar. Res.* 42, 943–956. doi: 10.1357/002224084788520684

Marie, B., Arivalagan, J., Mathéron, L., Bolbach, G., Berland, S., Marie, A., et al. (2017). Deep conservation of bivalve nacre proteins highlighted by shell matrix proteomics of the Unionoida *Elliptio complanata* and *Villosa lienosa*. *J. R. Soc. Interface* 14:20160846. doi: 10.1098/rsif.2016.0846

Marie, B., Joubert, C., Tayalé, A., Zanella-Cleón, I., Belliard, C., Piquemal, D., et al. (2012). Different secretory repertoires control the biomineralization processes of prism and nacre deposition of the pearl oyster shell. *Proc. Natl. Acad. Sci. U.S.A.* 109, 20986–20991. doi: 10.1073/pnas.1210552109

Marie, B., Le Roy, N., Zanella-Cléon, I., Becchi, M., and Marin, F. (2011). Molecular evolution of mollusc shell proteins: insights from proteomic analysis of the edible mussel *Mytilus*. *J. Mol. Evol.* 72, 531–546. doi: 10.1007/s00239-011-9451-6

Marin, F., Roy, N. L., and Marie, B. (2012). The formation and mineralizarion of mollusks shell. *Front. Biosci.* 4:1099–1125.

Miyamoto, H., Miyashita, T., Okushima, M., Nakano, S., Morita, T., and Matsushiro, A. (1996). A. carbonic anhydrase from the nacreous layer in oyster pearls. *Proc. Natl. Acad. Sci. U.S.A.* 93, 9657–9660. doi: 10.1073/pnas.93.18.9657

Miyamura, M., and Makido, T. (1958). Quality of the pearl examined in association with the graft tissues taken from various parts of the mantle. *B. Jpn. Soc. Sci. Fish.* 24, 441–444.

Miyazaki, Y., Nishida, T., Aoki, H., and Samata, T. (2010). Expression of genes responsible for biomineralization of *Pinctada fucata* during development. *Comp. Biochem. Physiol. B Biochem. Mol. Biol.* 155, 241–248. doi: 10.1016/j.cbpb.2009.11.009

Mizumoto, S. (1965). "Tansuishinjyu," in *Shinjyu Yousyoku Zensyo Hensui Iinnkai*, ed. Shinjyu Yousyoku Zensho (Tokyo: Zenkoku Shinjyu Yousyoku Gyogyoukumiai Rengoukai), 428–457. [in Japanese].

Moini, M., O'Halloran, A., Peters, A. M., France, C. A. M., Vicenzi, E. P., Dewitt, T. G., et al. (2014). Understanding irregular shell formation of *Nautilus* in aquaria: chemical composition and structural analysis. *Zoo. Biol.* 33, 285–294. doi: 10.1002/zoo.21132

Nishida, K., Ishimura, T., Suzuki, A., and Sasaki, T. (2012). Seasonal changes in the shell microstructure of the bloody clam, *Scapharca broughtonii* (Mollusca: Bivalvia: Arcidae). *Palaeogeogr. Palaeoclimatol. Palaeoecol.* 363–364, 99–108. doi: 10.1016/j.palaeo.2012.08.017

Nishida, K., Suzuki, A., Isono, R., Hayashi, M., Watanabe, Y., Yamamoto, Y., et al. (2015). Thermal dependency of shell growth, microstructure, and stable isotopes in laboratory-reared *Scapharca broughtonii* (Mollusca: Bivalvia). *Geochem. Geophys. Geosys.* 16, 2395–2408. doi: 10.1002/2014GC005634

Olson, I. C., Kozdon, R., Valley, J. W., and Gilbert, P. U. P. A. (2012). Mollusk shell nacre ultrastructure correlates with environmental temperature and pressure. *J. Am. Chem. Soc.* 134, 7351–7358. doi: 10.1021/ja210808s

Palmer, A. R. (1992). Calcification in marine molluscs: how costly is it? *Proc. Natl. Acad. Sci. U.S.A.* 89, 1379–1382. doi: 10.1073/pnas.89.4.1379

R Core Team (2020). *R: A Language and Environment for Statistical Computing*. Vienna: R Foundation for Statistical Computing.

Rogulja, D., and Irvine, K. D. (2005). Regulation of cell proliferation by a morphogen gradient. *Cell* 123, 449–461. doi: 10.1016/j.cell.2005.08.030

Samata, T., Hayashi, N., Kono, M., Hasegawa, K., Horita, C., and Akera, S. (1999). A new matrix protein family related to the nacreous layer formation of *Pinctada fucata*. *FEBS Lett.* 462, 225–229. doi: 10.1016/S0014-5793(99)01387-3

Saruwatari, K., Matsui, T., Mukai, H., Nagasawa, H., and Kogure, T. (2009). Nucleation and growth of aragonite crystals at the growth front of nacres in pearl oyster, *Pinctada fucata*. *Biomaterials* 30, 3028–3034. doi: 10.1016/j.biomaterials.2009.03.011

Sato, K., Kano, Y., Setiamarga, D. H. E., Watanabe, H. K., and Sasaki, T. (2020a). Molecular phylogeny of protobranch bivalves and systematic implications of their shell microstructure. *Zool. Scr.* 49, 458–472. doi: 10.1111/zsc.12419

Sato, K., Watanabe, H. K., Jenkins, R. G., and Chen, C. (2020b). Phylogenetic constraint and phenotypic plasticity in the shell microstructure of vent and seep pectinodontid limpets. *Mar. Biol.* 167:79. doi: 10.1007/s00227-020-03692-z

Setiamarga, D. H. E., Hirota, K., Yoshida, M., Takeda, Y., Kito, K., Ishikawa, M., et al. (2021). Hydrophilic shell matrix proteins of *Nautilus pompilius* and the

identification of a core set of conchiferan domains. *bioRxiv* [Preprint]. doi: 10.1101/2020.11.14.382804

Setiamarga, D. H. E., Shimizu, K., Kuroda, J., Inamura, K., Sato, K., Isowa, Y., et al. (2013). An in-silico genomic survey to annotate genes coding for early development-relevant signaling molecules in the pearl oyster, *Pinctada fucata*. *Zoolog. Sci.* 30, 877–888. doi: 10.2108/zsj.30.877

Shimizu, K., Iijima, M., Setiamarga, D. H. E., Sarashina, I., Kudoh, T., Asami, T., et al. (2013). Left-right asymmetric expression of *dpp* in the mantle of gastropods correlates with asymmetric shell coiling. *Evodevo* 4:15. doi: 10.1186/2041-9139-4-15

Shinomiya, Y., Iwanaga, S., Kohno, K., and Yamaguchi, T. (1999). Seasonal variations in carbohydrate-metabolizing enzyme activity and body composition of Japanese pearl oyster *Pinctada fucata* martensii in pearl culture. *Nippon Suisan Gakkaishi* 65, 294–299. doi: 10.2331/suisan.65.294

Spann, N., Harper, E. M., and Aldridge, D. C. (2010). The unusual mineral vaterite in shells of the freshwater bivalve *Corbicula fluminea* from the UK. *Naturwissenschaften* 97, 743–751. doi: 10.1007/s00114-010-0692-9

Sudo, S., Fujikawa, T., Nagakura, T., Ohkubo, T., Sakaguchi, K., Tanaka, M., et al. (1997). Structures of mollusc shell framework proteins. *Science* 387, 563–564. doi: 10.1038/42391

Suzuki, M., Murayama, E., Inoue, H., Ozaki, N., Tohse, H., Kogure, T., et al. (2004). Characterization of Prismalin-14, a novel matrix protein from the prismatic layer of the Japanese pearl oyster (*Pinctada fucata*). *Biochem. J.* 382, 205–213. doi: 10.1042/BJ20040319

Suzuki, M., Saruwatari, K., Kogure, T., Yamamoto, Y., Nishimura, T., Kato, T., et al. (2009). An acidic matrix protein, Pif, is a key macromolecule for nacre formation. *Science* 325, 1388–1390. doi: 10.1126/science.1173793

Suzuki, S., and Uozumi, S. (1979). The histochemical changes associated with the development of the organic membrane-shell in mussel, *Mytilus edulis* [in Japanese]. *Earth Sci.* 33, 200–207.

Takeuchi, T., and Endo, K. (2006). Biphasic and dually coordinated expression of the genes encoding major shell matrix proteins in the pearl oyster *Pinctada fucata*. *Mar. Biotechnol.* 8, 52–61. doi: 10.1007/s10126-005-5037-x

Takeuchi, T., Kawashima, T., Koyanagi, R., Gyoja, F., Tanaka, M., Ikuta, T., et al. (2012). Draft genome of the pearl oyster *Pinctada fucata*: a platform for understanding bivalve biology. *DNA Res.* 19, 117–130. doi: 10.1093/dnares/dss005

Takeuchi, T., Koyanagi, R., Gyoja, F., Kanda, M., Hisata, K., Fujie, M., et al. (2016). Bivalve-specific gene expansion in the pearl oyster genome: implications of adaptation to a sessile lifestyle. *Zool. Lett.* 2, 1–13. doi: 10.1186/s40851-016-0039-2

Takeuchi, T., Sarashina, I., Iijima, M., and Endo, K. (2008). In vitro regulation of $CaCO_3$ crystal polymorphism by the highly acidic molluscan shell protein Aspein. *FEBS Lett.* 582, 591–596. doi: 10.1016/j.febslet.2008.01.026

Taylor, J. D., and Layman, M. (1972). The mechanical properties of bivalve (Mollusca) shell structure. *Paleontology* 15, 73–87.

Taylor, J. D., Kennedy, W. J., and Hall, A. (1969). The shell structure and mineralogy of the bivalvia. introduction, Nuculacea-Trigonacea. *Bull. Brit. Mus. Nat. His. Zool.* 3, 1–125.

Taylor, J. D., Kennedy, W. J., and Hall, A. (1973). The shell structure and mineralogy of the Bivalvia. II. Lucinacea-Clavagellacea, Conclusions. *Bull. Brit. Mus. Nat. His. Zool.* 22, 253–284.

Tsukamoto, D., Sarashina, I., and Endo, K. (2004). Structure and expression of an unusually acidic matrix protein of pearl oyster shells. *Biochem. Biophys. Res. Commun.* 320, 1175–1180. doi: 10.1016/j.bbrc.2004.06.072

Vendrasco, M. J., Checa, A. G., and Kouchinsky, A. V. (2011). Shell microstructure of the early bivalve *Pojetaia* and the independent origin of nacre within the mollusca. *Palaeontology* 54, 825–850. doi: 10.1111/j.1475-4983.2011.01056.x

Vendrasco, M. J., Checa, A. G., Heimbrock, W. P., and Baumann, S. D. J. (2013). Nacre in molluscs from the ordovician of the Midwestern United States. *Geoscience* 3, 1–29. doi: 10.3390/geosciences3010001

Venturelli, O. S., El-Samad, H., and Murray, R. M. (2012). Synergistic dual positive feedback loops established by molecular sequestration generate robust bimodal response. *Proc. Natl. Acad. Sci. U.S.A* 109, E3324–E3333. doi: 10.1073/pnas.1211902109

Wada, K. (1961). The influence of the life-activity upon pearl formation in the pearl culture of *Pinctada martensii* (Dunker) II. The seasonal changes of crysta1 growth and luster of the pearl. *Bull. Natl. Pearl. Res. Lab.* 6, 586–606.

Wada, K. (1972). Nucleation and growth of aragonite crystals in the nacre of some bivalve molluscs. *Biomineralisation* 6, 141–159.

Wang, N., Kinoshita, S., Riho, C., Maeyama, K., Nagai, K., and Watabe, S. (2009). Quantitative expression analysis of nacreous shell matrix protein genes in the process of pearl biogenesis. *Comp. Biochem. Physiol. B Biochem. Mol. Biol.* 154, 346–350. doi: 10.1016/j.cbpb.2009.07.012

Weiner, S., Talmon, Y., and Traub, W. (1983). Electron diffraction of mollusc shell organic matrices and their relationship to the mineral phase. *Int. J. Biol. Macromol.* 5, 325–328. doi: 10.1016/0141-8130(83)90055-7

Yano, M., Nagai, K., Morimoto, K., and Miyamoto, H. (2007). A novel nacre protein N19 in the pearl oyster *Pinctada fucata*. *Biochem. Biophys. Res. Commun.* 362, 158–163. doi: 10.1016/j.bbrc.2007.07.172

Zhang, H., Chen, Y., and Chen, Y. (2012). Noise propagation in gene regulation networks involving interlinked positive and negative feedback loops. *PLoS One* 7:e51840. doi: 10.1371/journal.pone.0051840

Zhang, L., and He, M. (2011). Quantitative expression of shell matrix protein genes and their correlations with shell traits in the pearl oyster *Pinctada fucata*. *Aquaculture* 314, 73–79. doi: 10.1016/j.aquaculture.2011.01.039

Zhang, R., Xie, L., and Yan, Z. (2018). *Biomineralization Mechanism of the Pearl Oyster, Pinctada fucata*. Singapore: Springer.

Zhang, Y., Xie, L., Meng, Q., Jiang, T., Pu, R., Chen, L., et al. (2003).). A novel matrix protein participating in the nacre framework formation of pearl oyster, *Pinctada fucata*. *Comp. Biochem. Physiol. B Biochem. Mol. Biol.* 135, 565–573. doi: 10.1016/S1096-4959(03)00138-6

Conflict of Interest: The authors declare that the research was conducted in the absence of any commercial or financial relationships that could be construed as a potential conflict of interest.

Publisher's Note: All claims expressed in this article are solely those of the authors and do not necessarily represent those of their affiliated organizations, or those of the publisher, the editors and the reviewers. Any product that may be evaluated in this article, or claim that may be made by its manufacturer, is not guaranteed or endorsed by the publisher.